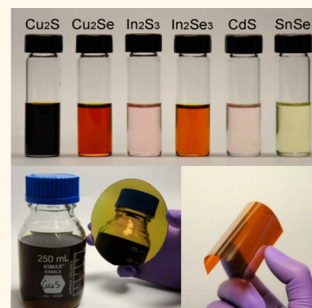


# Cosolvent Approach for Solution-Processable Electronic Thin Films

Zhaoyang Lin,<sup>†</sup> Qiyuan He,<sup>†</sup> Anxiang Yin,<sup>†</sup> Yuxi Xu,<sup>†</sup> Chen Wang,<sup>‡</sup> Mengning Ding,<sup>†</sup> Hung-Chieh Cheng,<sup>‡</sup> Benjamin Papandrea,<sup>†</sup> Yu Huang,<sup>‡,§</sup> and Xiangfeng Duan<sup>\*,†,§</sup>

<sup>†</sup>Department of Chemistry and Biochemistry, <sup>‡</sup>Department of Materials Science and Engineering, and <sup>§</sup>California NanoSystems Institute, University of California, Los Angeles, California 90095, United States

**ABSTRACT** Low-temperature solution-processable electronic materials are of considerable interest for large-area, low-cost electronics, thermoelectrics, and photovoltaics. Using a soluble precursor and suitable solvent to formulate a semiconductor ink is essential for large-area fabrication of semiconductor thin films. To date, it has been shown that hydrazine can be used as a versatile solvent to process a wide range of inorganic semiconductors. However, hydrazine is highly toxic and not suitable for large-scale manufacturing. Here we report a binary mixed solvent of amine and thiol for effective dispersion and dissolution of a large number of inorganic semiconductors including Cu<sub>2</sub>S, Cu<sub>2</sub>Se, In<sub>2</sub>S<sub>3</sub>, In<sub>2</sub>Se<sub>3</sub>, CdS, SnSe, and others. The mixed solvent is significantly less toxic and safer than hydrazine, while at the same time offering the comparable capability of formulating diverse semiconductor ink with a concentration as high as >200 mg/mL. We further show that such ink material can be readily processed into high-performance semiconducting thin films (Cu<sub>2</sub>S and Cu<sub>2</sub>Se) with the highest room-temperature conductivity among solution-based materials. Furthermore, we show that complex semiconductor alloys with tunable band gaps, such as CuIn(S<sub>x</sub>Se<sub>1-x</sub>)<sub>2</sub> (0 ≤ x ≤ 1), can also be readily prepared by simply mixing Cu<sub>2</sub>S, Cu<sub>2</sub>Se, In<sub>2</sub>S<sub>3</sub>, and In<sub>2</sub>Se<sub>3</sub> ink solutions in a proper ratio. Our study outlines a general strategy for the formulation of inorganic semiconductor ink for low-temperature processing of large-area electronic thin films on diverse substrates and can greatly impact diverse areas including flexible electronics, thermoelectrics, and photovoltaics.



**KEYWORDS:** solvent · solution process · semiconductor · thin films · flexible electronics

The ability to deposit and modulate conducting and semiconducting films on various substrates, including silicon and plastic, is of central importance for contemporary and future solid-state electronics and photovoltaics.<sup>1–5</sup> For example, the semiconducting thin film of copper indium gallium selenide (CIGS) represents the most efficient material for thin film solar cells, with the highest solar-to-electricity power conversion efficiency of around 20% and greatly reduced active material compared with the traditional crystalline silicon solar cells.<sup>6</sup> Conducting metal oxide thin films are widely used as the transparent electrodes or active components in touch screens and photovoltaics, which require a high electrical conductivity.<sup>7–9</sup> Current approaches to these thin films typically rely on high-temperature chemical vapor deposition (CVD) or high-vacuum physical vapor deposition (PVD) processes, which are usually too costly and require a too high processing temperature, and are not typically compatible with the growing demand of low-cost and large-area

electronics, such as the emerging wearable devices. For example, to fabricate a CIGS thin film on desired substrates, the most common vacuum-based process is to co-evaporate or cosputter copper, indium, and gallium onto the substrate (e.g., glass), followed by a thermal annealing process in a selenium vapor.<sup>6,10</sup> The vacuum deposition and high-temperature annealing in toxic vapor are not favored from a cost and safety point of view. Additionally, preparing thin films using CVD or PVD processes over a large area has always been a challenge due to the limited size of the vacuum chamber and furnace and uniformity of the heating zone. As a result, solution processes, with the potential advantages of low cost, low temperature, and compatibility with plastic substrates, have emerged as an attractive approach for next-generation flexible electronic devices, wearable computers, and large-area displays.<sup>2,11–13</sup>

A few solution-based deposition processes, such as electrophoretic deposition and chemical bath deposition, have been

\* Address correspondence to xduan@chem.ucla.edu.

Received for review February 6, 2015 and accepted April 6, 2015.

Published online April 13, 2015  
10.1021/acsnano.5b00886

© 2015 American Chemical Society

successfully used to form semiconductor films for electronic device applications.<sup>12,14–16</sup> A CdS thin film grown by chemical bath deposition with a multidip method has yielded a carrier mobility of  $4.64 \text{ cm}^2 \cdot \text{V}^{-1} \cdot \text{s}^{-1}$ .<sup>15</sup> However, although these methods are considered to be solution-based, generally they are not as high-throughput as the standard spin-coating or various printing processes that require a truly soluble precursor and a suitable solvent to formulate a processable ink material.

To this end, the deposition of surface-functionalized nanocrystals using spin-coating or printing processes has become a potential alternative approach due to the excellent dispersibility and controlled properties.<sup>4</sup> With the advance in material synthesis at the nanoscale, zero dimensional (0D) (e.g., quantum dots), one-dimensional (1D) (e.g., nanowires and nanotubes), and two-dimensional (2D) nanostructures (e.g., nanoplates and nanosheets) have been synthesized with nearly perfect crystalline structures.<sup>17–25</sup> These nanostructures can often be dispersed in a solution to form a stable and easy-to-handle colloidal ink to allow solution processing with general coating methods. These solution processes offer the advantages of low temperature, low cost, and excellent scalability for large-area electronics on glass or plastic substrates.<sup>4,26</sup> However, the preparation of these crystalline nanostructures usually involves sophisticated synthetic control of the shape/size, complicated surface modification, and a large quantity of organic waste, which all add to the complexity and cost of the overall process.<sup>27,28</sup> Ideally, the direct dissolution of semiconductors in a proper solvent and recovery on a substrate is one of the most favorable and efficient methods for the fabrication of large-area thin films with greatly simplified procedures and reduced cost. Unfortunately, due to the strong covalent bonding in most inorganic semiconductors, solvents that can be readily used to process these materials were lacking until hydrazine was reported to be capable of dissolving  $\text{SnS}_2$  and  $\text{Sn(S, Se)}_2$  with the assistance of excess chalcogen (S or Se) in 2004, which is also the sole general solvent for various semiconductors including  $\text{In}_2\text{Se}_3$ ,  $\text{Cu}_2\text{S}$ ,  $\text{CuInSe}_2$ ,  $\text{Cu(In}_{1-x}\text{Ga}_x\text{)Se}_2$ , and so on.<sup>2,29</sup> However, the high toxicity and instability of anhydrous hydrazine are extremely unfavorable in practical applications and massive production processes. Seeking an alternative solvent for semiconductor ink materials has been an important research direction in the past decade.<sup>30,31</sup> For example, a non-hydrazine-based solvent mixture has been recently explored as an effective solvent to dissolve chalcogen and  $\text{As}_2\text{X}_3$ ,  $\text{Sb}_2\text{X}_3$ , and  $\text{Bi}_2\text{X}_3$  ( $\text{X} = \text{S, Se, Te}$ ).<sup>32,33</sup>

Here we report a general cosolvent approach for the formulation of a wide range of inorganic semiconductor inks for high-performance electronic thin films. We have previously shown that a cosolvent approach

can be used to exfoliate and disperse a wide range of two-dimensional layered materials in a simple mixture solvent of water and alcohols.<sup>34</sup> Here we show that a mixture of amine and thiol can function as a general solvent to dissolve a large number of inorganic semiconductors, including  $\text{Cu}_2\text{S}$ ,  $\text{Cu}_2\text{Se}$ ,  $\text{In}_2\text{S}_3$ ,  $\text{In}_2\text{Se}_3$ ,  $\text{CdS}$ ,  $\text{SnSe}$ , and more. With this approach, high-concentration semiconductor ink ( $>200 \text{ mg/mL}$ ) can be produced at room temperature and atmospheric pressure and be used to prepare semiconductor thin films on  $\text{SiO}_2/\text{Si}$  wafer, glass, and plastic substrates with extremely high uniformity over large areas. Electrical transport studies of the resulting  $\text{Cu}_2\text{S}$  and  $\text{Cu}_2\text{Se}$  thin films demonstrate the highest conductivity compared with all of those prepared by other solution methods, including nanocrystal deposition and chemical bath deposition, demonstrating the superior performance of our solution-processed semiconductor thin films. Furthermore, the cosolvent approach can also be used to process many other significant semiconductors, such as  $\text{CuIn(S}_x\text{Se}_{1-x})_2$  ( $0 \leq x \leq 1$ ),  $\text{SnS}$ ,  $\text{CdSe}$ ,  $\text{ZnSe}$ , and  $\text{MoS}_2$ . The capability to process semiconductors at room temperature and atmospheric pressure using a simple “dissolve and recover” solution process, with a relatively safe solvent, is an exciting advancement and offers great opportunities in the facile fabrication of semiconductor thin films for large-area high-performance electronics, thermoelectrics, and photovoltaics with high throughput, greatly reduced cost, and improved safety.

## RESULTS AND DISCUSSION

Our studies demonstrate that amine or thiol alone could not dissolve the semiconductor powders. Solid could be identified in both solutions when  $\text{Cu}_2\text{S}$  and  $\text{Cu}_2\text{Se}$  powder were added into amine without thiol (or thiol without amine). The  $\text{Cu}_2\text{Se}$  particles settle down at the bottom of the vial, while  $\text{Cu}_2\text{S}$  powder is suspended in the liquid due to its ultrafine nature (Figure 1a). With the addition of a small amount of thiol ( $\sim 10\%$  in volume), the powder starts to dissolve immediately and the liquid quickly turns dark for  $\text{Cu}_2\text{S}$  and brown for  $\text{Cu}_2\text{Se}$ . After stirring for 10 min, a clear dark  $\text{Cu}_2\text{S}$  and a brown  $\text{Cu}_2\text{Se}$  solution are obtained without any precipitate that can be identified by the naked eye (Figure 1b), indicating a complete dissolution. The dissolution power of the mixed amine–thiol solvent is attributed to the  $\text{RS}^-$  species existing in the mixture, which can bind to the metal ions. The fast ink preparation process is of great importance in terms of the fabrication efficiency, which is crucial in industrial processes. Ultraviolet–visible (UV–vis) studies show two absorption peaks for both solutions (with an equal concentration of Cu), at around 400 and 520 nm, respectively (Figure 1c). The absorption in the UV region is generally much higher than that in visible light, which is partially due to the strong absorption of UV light from the solvent itself

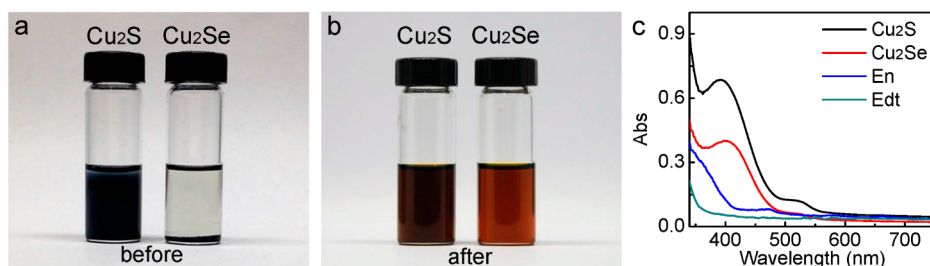


**Figure 1.** Characterization of the semiconductor ink solutions. (a) Photographs of the semiconductor powder in ethylenediamine before the addition of ethanedithiol. (b) Photographs of the semiconductor solutions after the addition of ethanedithiol. (c) UV-vis spectra for the diluted  $\text{Cu}_2\text{S}$ ,  $\text{Cu}_2\text{Se}$  ink solutions, ethylenediamine (En), and ethanedithiol (Edt), respectively.

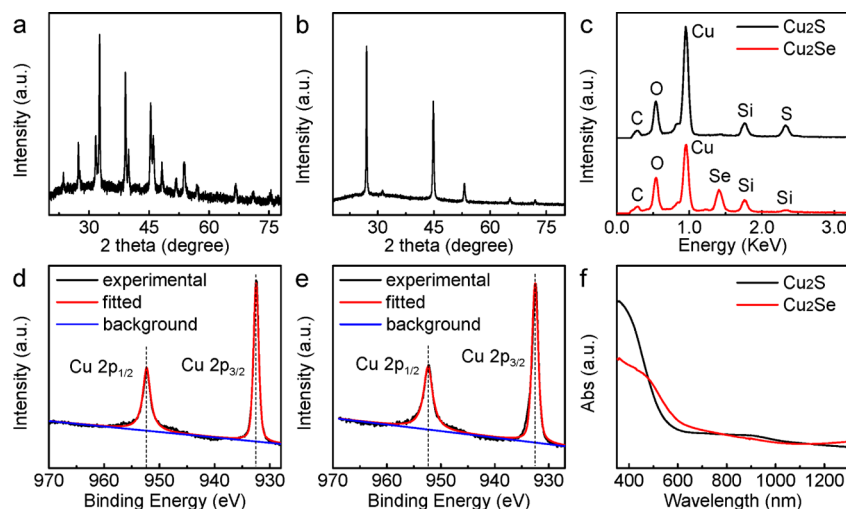


**Figure 2.** Characterization of the recovered  $\text{Cu}_2\text{S}$  and  $\text{Cu}_2\text{Se}$  thin films. (a, b) Powder X-ray diffraction pattern of the recovered thin films on glass substrates for  $\text{Cu}_2\text{S}$  (a) and  $\text{Cu}_2\text{Se}$  (b), respectively. (c) Energy dispersive X-ray spectra for recovered thin films. (d, e) X-ray photoelectron microscopy for  $\text{Cu}_2\text{S}$  (d) and  $\text{Cu}_2\text{Se}$  (e) film on the  $\text{SiO}_2/\text{Si}$  substrate. (f) UV-vis spectra for  $\text{Cu}_2\text{S}$  and  $\text{Cu}_2\text{Se}$  films on the glass substrate.

(both amine and thiol) (Figure 1c). The overall shape of the absorption spectra for both solutions is quite similar other than a slight difference in peak position. Despite that, the overall absorption of the  $\text{Cu}_2\text{S}$  solution is generally higher than that of the  $\text{Cu}_2\text{Se}$  solution and thus appears darker.

With the formation of soluble semiconductor ink, the corresponding semiconductor thin films could be readily prepared by the deposition of  $\text{Cu}_2\text{S}$  and  $\text{Cu}_2\text{Se}$  solutions on various substrates *via* a spin-coating or drop-casting method followed by a thermal annealing step. The powder X-ray diffraction (XRD) patterns of the resulting thin films show the pure phase of tetragonal  $\text{Cu}_2\text{S}$  and cubic  $\text{Cu}_2\text{Se}$ , respectively (Figure 2a,b). The energy-dispersive X-ray spectroscopy (EDS) confirms the existence of Cu and S in  $\text{Cu}_2\text{S}$  and Cu and Se in  $\text{Cu}_2\text{Se}$ , with the Cu to S and Cu to Se ratio around 2:1, indicating the presence of Cu(I) in the thin films (Figure 2c). X-ray photoelectron spectroscopy (XPS) was also conducted to probe the oxidation state of Cu in the thin films. The XPS spectra for both  $\text{Cu}_2\text{S}$  and  $\text{Cu}_2\text{Se}$  films exhibit two peaks matching well with Cu(I) 2p binding energy (Figure 2d,e). Furthermore, the

peaks can be perfectly fit with the sole existence of Cu(I) species without any shoulder peaks, demonstrating that there is no or a negligible amount of Cu(II) species in the prepared thin films. The UV-vis spectrum shows the indirect and direct band gap absorption edge at around 600 and 1000 nm for  $\text{Cu}_2\text{S}$  (Figure 2f), which agrees well with the previously reported data.<sup>35</sup> The  $\text{Cu}_2\text{Se}$  has a similar spectrum with the indirect and direct band gap absorption at around 700 and 1000 nm.<sup>36</sup> Together, these studies demonstrate that these solution-processed thin films exhibit the expected  $\text{Cu}_2\text{S}$  and  $\text{Cu}_2\text{Se}$  crystalline structures with no sign of the oxidation of Cu(I).

Using the semiconductor ink, thin films of  $\text{Cu}_2\text{S}$  and  $\text{Cu}_2\text{Se}$  can be readily prepared on the standard 4 in.  $\text{SiO}_2/\text{Si}$  substrate *via* a simple spin-coating process. Compared with the conventional CVD or PVD process, the solution-processed thin films are easily scalable. Importantly, with the truly soluble precursor in the solution, the prepared thin films show a mirror-like surface (Figure 3a,d), indicating excellent uniformity and smoothness of the resulting films. The scanning electron microscopy (SEM) studies revealed closely

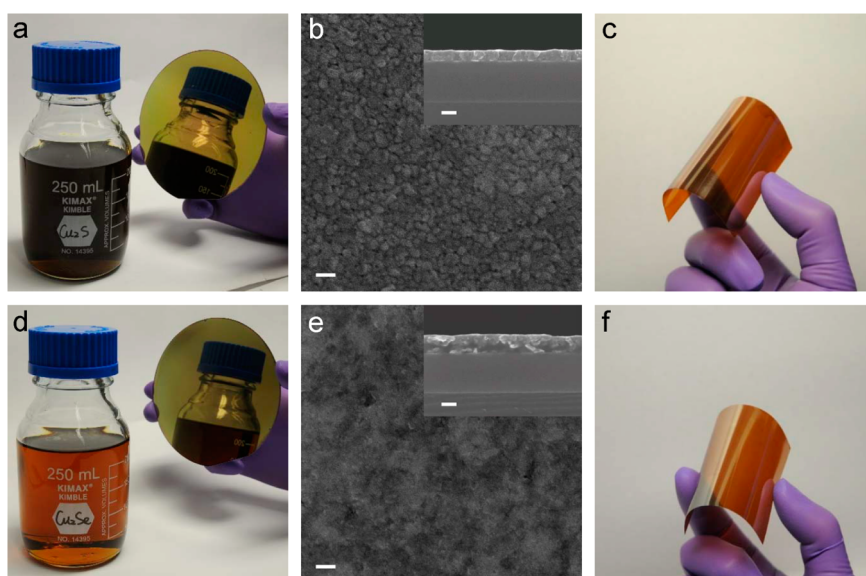


**Figure 3.** Structural characterization of the recovered  $\text{Cu}_2\text{S}$  and  $\text{Cu}_2\text{Se}$  thin films. (a and d) Photographs of the  $\text{Cu}_2\text{S}$  (a) and  $\text{Cu}_2\text{Se}$  (d) ink solution and as-deposited thin films on a standard 4 in.  $\text{SiO}_2/\text{Si}$  wafer with a mirror-like surface. (b and e) SEM images of  $\text{Cu}_2\text{S}$  (b) and  $\text{Cu}_2\text{Se}$  (e) thin films. Inset is the cross-sectional SEM image for the respective thin film. Scale bar is 100 nm for all images. (c and f) Photographs of the as-deposited  $\text{Cu}_2\text{S}$  (c) and  $\text{Cu}_2\text{Se}$  (f) thin films on the flexible polyimide substrate.

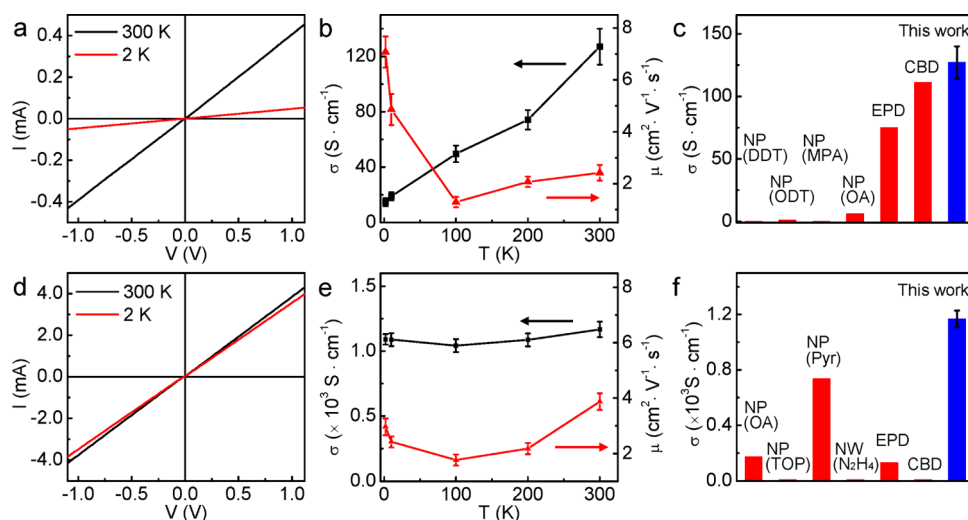


**Figure 4.** Electrical characterization of the prepared  $\text{Cu}_2\text{S}$  and  $\text{Cu}_2\text{Se}$  thin films. (a)  $I$ – $V$  curve for the  $\text{Cu}_2\text{S}$  thin film at 300 and 2 K. (b) Temperature dependence of the mobility and conductivity of the  $\text{Cu}_2\text{S}$  thin film in the range from 2 to 300 K. (c) Comparison of the conductivity among  $\text{Cu}_2\text{S}$  thin films from typical solution-based methods. NP: nanoparticle. DDT: dodecanethiol.<sup>45</sup> ODT: octadecanethiol.<sup>46</sup> MPA: mercaptopropionic acid.<sup>44</sup> OA: oleylamine.<sup>37</sup> EPD: electrophoretic deposition.<sup>37</sup> CBD: chemical bath deposition.<sup>41</sup> (d)  $I$ – $V$  curve for the  $\text{Cu}_2\text{Se}$  thin film at 300 and 2 K. (e) Temperature dependence of the mobility and conductivity of the  $\text{Cu}_2\text{Se}$  thin film in the range from 2 to 300 K. (f) Comparison of the conductivity among  $\text{Cu}_2\text{Se}$  thin films from typical solution-based methods. NP: nanoparticle. NW: nanowire.<sup>39</sup> OA: oleylamine.<sup>38</sup> TOP: trioctylphosphine.<sup>40</sup> Pyr: pyridine.<sup>43</sup> EPD: electrophoretic deposition.<sup>42</sup> CBD: chemical bath deposition.<sup>36</sup>

packed nanoparticles in the  $\text{Cu}_2\text{S}$  thin film (Figure 3b), while the nanoparticle nature in the  $\text{Cu}_2\text{Se}$  film is less obvious (Figure 3e). The cross sectional SEM images confirmed the flat and compact nature of the prepared thin films on the  $\text{SiO}_2/\text{Si}$  substrate (Figure 3b,e). Together, our studies show that high-quality  $\text{Cu}_2\text{S}$  and  $\text{Cu}_2\text{Se}$  thin films can be prepared on the substrate with a high degree of uniformity and the absence of significant voids. To take a step further, we have deposited uniform  $\text{Cu}_2\text{S}$  (Figure 3c) and  $\text{Cu}_2\text{Se}$  (Figure 3f) thin films

on a flexible plastic substrate *via* the same spin-coating process, which demonstrates their potential applications in flexible and wearable electronics.

To probe the electronic properties of the resulting  $\text{Cu}_2\text{S}$  and  $\text{Cu}_2\text{Se}$  thin films, we have fabricated two terminal devices with Ti/Au (50 nm/50 nm) thin film electrodes. Electrical transport measurements show linear  $I$ – $V$  behavior at both 300 and 2 K for both  $\text{Cu}_2\text{S}$  (Figure 4a) and  $\text{Cu}_2\text{Se}$  (Figure 4d) thin films, indicating an ohmic contact with the Ti/Au electrodes. We have

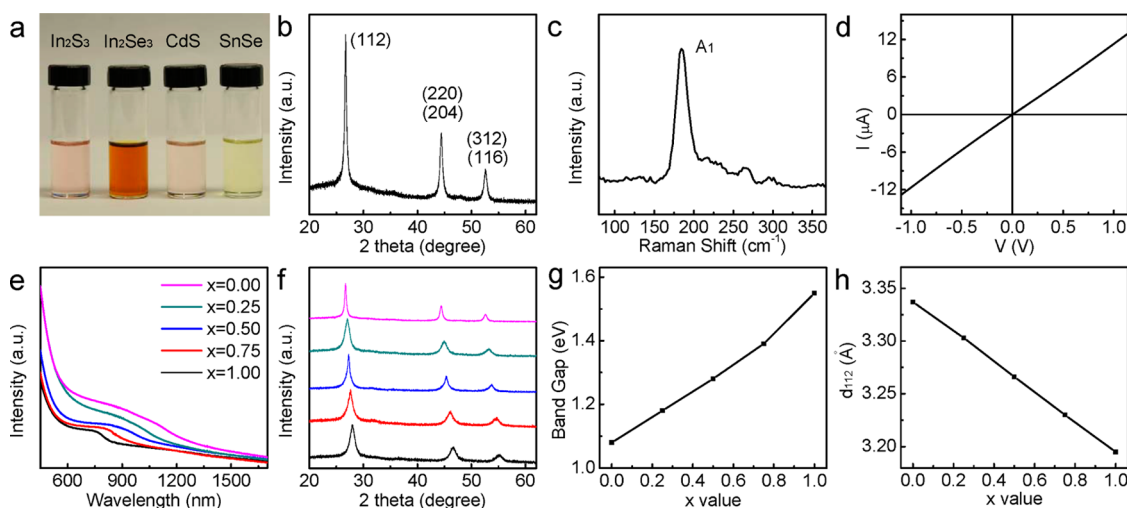


**Figure 5.** Solution processing of ternary and quaternary semiconductor alloy thin films. (a) Photograph of the  $\text{In}_2\text{S}_3$ ,  $\text{In}_2\text{Se}_3$ , CdS, and SnSe ink solutions formulated with the cosolvent approach. (b) XRD pattern of the  $\text{CuInSe}_2$  thin films prepared by mixing a  $\text{Cu}_2\text{Se}$  and  $\text{In}_2\text{Se}_3$  ink solution with a 1:1 molar ratio, exhibiting the pure phase. (c) Raman spectroscopy for the prepared  $\text{CuInSe}_2$  thin film, showing the expected  $A_1$  mode. (d)  $I$ - $V$  behavior for the  $\text{CuInSe}_2$  film measured at room temperature. The geometry for the device is width/length (W/L) = 1:2. (e) Optical absorption for  $\text{CuIn}(\text{S}_x\text{Se}_{1-x})_2$  films with a tunable  $x$  value, fabricated by mixing  $\text{Cu}_2\text{S}$ ,  $\text{Cu}_2\text{Se}$ ,  $\text{In}_2\text{S}_3$ , and  $\text{In}_2\text{Se}_3$  ink solutions with different ratios. (f) X-ray diffraction peak evolution for the  $\text{CuIn}(\text{S}_x\text{Se}_{1-x})_2$  films with tunable  $x$  value in (e). (g) Compositional dependence of the optical band gap energy for  $\text{CuIn}(\text{S}_x\text{Se}_{1-x})_2$  films. (h) Compositional dependence of the crystal lattice constant for the (112) plane in  $\text{CuIn}(\text{S}_x\text{Se}_{1-x})_2$  films.

further conducted temperature-dependent measurements to determine the conductivity and carrier mobility of the semiconductor thin films as a function of temperature (Figure 4b,e). For the  $\text{Cu}_2\text{S}$  thin film, the conductivity decreases with decreasing temperature in the range 300 to 2 K (Figure 4b), showing a typical semiconductor behavior.<sup>37</sup> During the cooling process, the carrier mobility initially decreases and then increases below 100 K, which is also a common behavior of  $\text{Cu}_2\text{S}$ . For the  $\text{Cu}_2\text{Se}$  thin film, the overall conductivity does not change significantly with the temperature variation (Figure 4e). The carrier mobility in  $\text{Cu}_2\text{Se}$  shows similar behavior to that of  $\text{Cu}_2\text{S}$ , which decreases first and then increases at low temperature. More importantly, the conductivities of the thin films ( $127 \text{ S}\cdot\text{cm}^{-1}$  for  $\text{Cu}_2\text{S}$  and  $1168 \text{ S}\cdot\text{cm}^{-1}$  for  $\text{Cu}_2\text{Se}$ ) prepared from our semiconductor ink solution are the highest among all of the solution-processed thin films for both  $\text{Cu}_2\text{S}$  (Figure 4c) and  $\text{Cu}_2\text{Se}$  (Figure 4f).<sup>36–46</sup> The carrier mobility values ( $2.4 \text{ cm}^2\cdot\text{V}^{-1}\cdot\text{s}^{-1}$  for  $\text{Cu}_2\text{S}$  and  $3.9 \text{ cm}^2\cdot\text{V}^{-1}\cdot\text{s}^{-1}$  for  $\text{Cu}_2\text{Se}$ ) are also among the highest ones reported for solution-processed  $\text{Cu}_2\text{S}$  and  $\text{Cu}_2\text{Se}$  films. We attribute the superior electrical performance to the truly soluble precursor in the solution that enables a highly uniform, compact, and void-free thin film. Although previous studies have shown a quite high conductivity in the  $\text{Cu}_2\text{S}$  films from electrochemical deposition and chemical bath deposition (Figure 4c),<sup>37,41</sup> these approaches are intrinsically limited due to the difficulties in scalable processing of large-area thin films. In another case, it has been shown that the  $\text{Cu}_2\text{Se}$  thin films have been prepared from the deposition of pyridine-modified nanocrystals with a

decent electrical performance (Figure 4f),<sup>43</sup> which is complicated by sophisticated nanocrystal shape and size control. Additionally, postsynthesis or postdeposition surface functionalization or ligand exchange is usually required to activate the electrical performance, which introduces extra complexity and adds to the fabrication cost.<sup>27,47</sup> The ultimate goal of solution processes is to prepare the large-area high-performance thin film with a low cost and simple procedure.<sup>4,11</sup> To this end, our strategy to use the directly dissolved semiconductor ink, at room temperature and atmospheric pressure, followed by spin coating or other high-efficiency deposition methods in industry, such as printing or roll-to-roll coating process, is the most desirable process.

Importantly, our cosolvent approach to formulate inorganic semiconductor ink is general and can be extended to many other materials. For example, we have demonstrated that  $\text{In}_2\text{S}_3$ ,  $\text{In}_2\text{Se}_3$ , CdS, and SnSe can also be dissolved in the same solvent, with a high concentration ( $>200 \text{ mg/mL}$ ) (Figure 5a). Other materials, such as SnS, CdSe, ZnSe, and  $\text{MoS}_2$ , are also processable using the binary solvent, while with a lower solubility. To extend the potential application of our semiconductor ink, we have shown that by mixing an equal molar amount of  $\text{Cu}_2\text{Se}$  and  $\text{In}_2\text{Se}_3$  ink solutions we can readily prepare high-quality thin films of  $\text{CuInSe}_2$ , the most popular material used in thin film solar cells. Importantly, the resulting  $\text{CuInSe}_2$  film exhibits a pure crystal phase as confirmed by XRD (Figure 5b) and Raman spectroscopy (Figure 5c), with a similar mirror-like reflection to the  $\text{Cu}_2\text{S}$  and  $\text{Cu}_2\text{Se}$  films. Our studies also show the electrical performance

of the  $\text{CuInSe}_2$  film is comparable to previously reported results (Figure 5d).<sup>48</sup> Similarly, more complex alloy  $\text{CuIn}(\text{S}_x\text{Se}_{1-x})_2$  ( $0 \leq x \leq 1$ ) films can be produced. Importantly, with our approach, the exact composition of the resulting  $\text{CuIn}(\text{S}_x\text{Se}_{1-x})_2$  ( $0 \leq x \leq 1$ ) thin films can be readily tuned by varying the mixing ratio of  $\text{Cu}_2\text{S}/\text{Cu}_2\text{Se}$  and  $\text{In}_2\text{S}_3/\text{In}_2\text{Se}_3$ , which is fairly difficult to achieve in nanocrystals, chemical bath deposition, and physical vapor deposition. The  $\text{CuIn}(\text{S}_x\text{Se}_{1-x})_2$  ( $0 \leq x \leq 1$ ) thin films show a tunable band gap absorption (Figure 5e,g) and a crystal structure (Figure 5f,h). Varying the content of S and Se results in a series of alloys between  $\text{CuInS}_2$  and  $\text{CuInSe}_2$  with controllable composition and property. The facile mixing method could significantly simplify the fabrication process of complex  $\text{CuIn}(\text{S}_x\text{Se}_{1-x})_2$  ( $0 \leq x \leq 1$ ) material and thus reduce the overall complexity and cost. Therefore, the truly soluble precursor of semiconductors in amine–thiol cosolvent can offer exciting opportunities in the practical fabrication of semiconductor-based electronics and photovoltaics.

## CONCLUSIONS

In summary, we have reported a general solution process for the facile fabrication of various high-performance semiconductor thin films by using an amine–thiol cosolvent. The cosolvent could dissolve semiconductors at room temperature and atmospheric pressure as a solution-processable ink material for large-area fabrication of high-performance

electronic thin films. We show this method can be used to process a wide range of semiconductors, including  $\text{Cu}_2\text{S}$ ,  $\text{Cu}_2\text{Se}$ ,  $\text{In}_2\text{S}_3$ ,  $\text{In}_2\text{Se}_3$ ,  $\text{CdS}$ ,  $\text{SnSe}$ ,  $\text{SnS}$ ,  $\text{CdSe}$ ,  $\text{ZnSe}$ , and  $\text{MoS}_2$ . The amine–thiol cosolvent is safer and more accessible than the toxic hydrazine solvent. Using the semiconductor ink through a simple spin-coating process, we show highly uniform mirror-like thin films could be prepared on diverse substrates, including silicon, glass, and plastic with a room-temperature conductivity of  $127 \text{ S} \cdot \text{cm}^{-1}$  for  $\text{Cu}_2\text{S}$  and  $1168 \text{ S} \cdot \text{cm}^{-1}$  for  $\text{Cu}_2\text{Se}$ , respectively. The obtained conductivities for  $\text{Cu}_2\text{S}$  and  $\text{Cu}_2\text{Se}$  thin films are the highest among all solution-processed  $\text{Cu}_2\text{S}$  and  $\text{Cu}_2\text{Se}$  thin films, including nanocrystal deposition and chemical bath deposition. Furthermore, many other interesting complex materials, like  $\text{CuIn}(\text{S}_x\text{Se}_{1-x})_2$  ( $0 \leq x \leq 1$ ), can also be processed by simply mixing precursor solutions in a proper molar ratio. Together, the facile dissolution process at room temperature and atmospheric pressure greatly simplify the ink formulation process and avoid the massive production of organic waste in nanocrystals synthesis, which is of great significance in practical applications. Our study defines a general strategy for the formulation of a wide range of inorganic semiconductor ink using a safe solvent at room temperature and atmospheric pressure. It can enable the construction of low-cost, large-area, and high-performance electronic thin films on diverse substrates for future flexible electronics, thermoelectrics, and photovoltaics.

## EXPERIMENTAL METHODS

**Chemicals.** Ethylenediamine ( $\text{H}_2\text{NCH}_2\text{CH}_2\text{NH}_2$ , >99%), ethanedithiol ( $\text{HSCH}_2\text{CH}_2\text{SH}$ , >98+%), copper(I) sulfide ( $\text{Cu}_2\text{S}$ , >99.5%), indium sulfide ( $\text{In}_2\text{S}_3$ , >99.95%), and indium selenide ( $\text{In}_2\text{Se}_3$ , >99.99%) were all purchased from Alfa-Aesar. Copper(I) selenide ( $\text{Cu}_2\text{Se}$ , >99.95%), cadmium sulfide ( $\text{CdS}$ , synthesis grade, fluffy powder), and tin(II) selenide ( $\text{SnSe}$ , >99.995%) were all purchased from Sigma-Aldrich. All the chemicals were used as received without further purification.

**Dissolution of Semiconductors.** To prepare typical semiconductor ink solutions, 100 mg of semiconductor powder ( $\text{Cu}_2\text{S}$ ,  $\text{Cu}_2\text{Se}$ ,  $\text{CdS}$ ,  $\text{In}_2\text{S}_3$ ,  $\text{In}_2\text{Se}_3$ ,  $\text{SnSe}$ ) was weighed and transferred to glass vials. Two mL of ethylenediamine was added into the vial followed by the addition of 0.2 mL of ethanedithiol in a nitrogen-filled glovebox. After 10 min of magnetic stirring for  $\text{Cu}_2\text{S}$ ,  $\text{Cu}_2\text{Se}$ , and  $\text{CdS}$  (and longer stirring for  $\text{In}_2\text{S}_3$ ,  $\text{In}_2\text{Se}_3$ , and  $\text{SnSe}$ ), a clear solution formed, indicating the complete dissolution. A gentle warming during the dissolution (*e.g.*, 40 °C on a hot plate) can facilitate the process. All of the above processes were done in a nitrogen-filled glovebox.

**Deposition of Semiconductor Thin Films.** Before the deposition, the obtained semiconductor inks were passed through a 0.45  $\mu\text{m}$  syringe filter to remove all of the possible impurities. The 300 nm  $\text{SiO}_2/\text{Si}$  substrate was used after the repeated wash with acetone and IPA followed by a 5 min oxygen plasma treatment. Then 20  $\mu\text{L}$  of ink solution was spin coated onto the silicon substrate with a speed of 2500 rpm for 60 s inside the glovebox. Then the coated substrate was heated on a hot plate at 300 °C for 1 h with a slow ramp time of 30 min or more. All of the processes were performed in a nitrogen-filled glovebox.

**Device Fabrication.** For the Hall effect measurement, small Ti/Au (50 nm/50 nm) electrodes were deposited onto the four corners of the patterned square films with a mask using the e-beam evaporator. The sheet resistance was calculated based on the van der Pauw method.

**Characterization.** Characterizations were carried out using scanning electron microscopy (SEM, JEOL JSM-6700F FE-SEM) with energy dispersive X-ray spectroscopy (EDAX), X-ray diffraction (XRD, Panalytical X'Pert Pro X-ray powder diffractometer), UV–vis–NIR spectroscopy (Shimadzu 3100 PC), Raman spectroscopy (Horiba, 514 nm laser wavelength), and X-ray photoelectron spectroscopy (XPS, AXIS Ultra DLD). The Hall measurements were performed in a PPMS (Quantum Design) cooled by liquid helium. Other transport characteristics measurements were conducted with a probe station and a computer-controlled analogue-to-digital converter at room temperature.

**Conflict of Interest:** The authors declare no competing financial interest.

**Acknowledgment.** We thank the support of the National Science Foundation EFRI-1433541.

## REFERENCES AND NOTES

- Forrest, S. R. Ultrathin Organic Films Grown by Organic Molecular Beam Deposition and Related Techniques. *Chem. Rev.* **1997**, *97*, 1793–1896.
- Mitzi, D. B.; Kosbar, L. L.; Murray, C. E.; Copel, M.; Afzali, A. High-Mobility Ultrathin Semiconducting Films Prepared by Spin Coating. *Nature* **2004**, *428*, 299–303.

3. Qing, C.; Hoon-sik, K.; Pimparkar, N.; Kulkarni, J. P.; Congjun, W.; Moonsub, S.; Roy, K.; Alam, M. A.; Rogers, J. A. Medium-Scale Carbon Nanotube Thin-Film Integrated Circuits on Flexible Plastic Substrates. *Nature* **2008**, *454*, 495–500.
4. Talapin, D. V.; Lee, J. S.; Kovalenko, M. V.; Shevchenko, E. V. Prospects of Colloidal Nanocrystals for Electronic and Optoelectronic Applications. *Chem. Rev.* **2010**, *110*, 389–458.
5. Liu, X. Q.; Liu, X.; Wang, J. L.; Liao, C. N.; Xiao, X. H.; Guo, S. S.; Jiang, C. Z.; Fan, Z. Y.; Wang, T.; Chen, X. S.; *et al.* Transparent, High-Performance Thin-Film Transistors with an InGaZnO/Aligned-SnO<sub>2</sub>-Nanowire Composite and Their Application in Photodetectors. *Adv. Mater.* **2014**, *26*, 7399–7404.
6. Stanbery, B. J. Copper Indium Selenides and Related Materials for Photovoltaic Devices. *Crit. Rev. Solid State Mater. Sci.* **2002**, *27*, 73–117.
7. Wu, W. Z.; Wen, X. N.; Wang, Z. L. Taxel-Addressable Matrix of Vertical-Nanowire Piezotronic Transistors for Active and Adaptive Tactile Imaging. *Science* **2013**, *340*, 952–957.
8. You, J. B.; Hong, Z. R.; Yang, Y.; Chen, Q.; Cai, M.; Song, T. B.; Chen, C. C.; Lu, S. R.; Liu, Y. S.; Zhou, H. P.; *et al.* Low-Temperature Solution-Processed Perovskite Solar Cells with High Efficiency and Flexibility. *ACS Nano* **2014**, *8*, 1674–1680.
9. Zhou, N. J.; Buchholz, D. B.; Zhu, G.; Yu, X. G.; Liu, H.; Facchetti, A.; Marks, T. J.; Chang, R. P. H. Ultraflexible Polymer Solar Cells Using Amorphous Zinc-Indium-Tin Oxide Transparent Electrodes. *Adv. Mater.* **2014**, *26*, 1098–1104.
10. Repins, I.; Contreras, M. A.; Egaas, B.; DeHart, C.; Scharf, J.; Perkins, C. L.; To, B.; Noufi, R. 19.9%-Efficient ZnO/CdS/CuInGaSe<sub>2</sub> Solar Cell with 81.2% Fill Factor. *Prog. Photovoltaics* **2008**, *16*, 235–239.
11. Sun, Y. G.; Rogers, J. A. Inorganic Semiconductors for Flexible Electronics. *Adv. Mater.* **2007**, *19*, 1897–1916.
12. Singh, A.; English, N. J.; Ryan, K. M. Highly Ordered Nanorod Assemblies Extending over Device Scale Areas and in Controlled Multilayers by Electrophoretic Deposition. *J. Phys. Chem. B* **2013**, *117*, 1608–1615.
13. Schwartz, G.; Tee, B. C. K.; Mei, J. G.; Appleton, A. L.; Kim, D. H.; Wang, H. L.; Bao, Z. N. Flexible Polymer Transistors with High Pressure Sensitivity for Application in Electronic Skin and Health Monitoring. *Nat. Commun.* **2013**, *4*, 1859.
14. Redinger, D.; Subramanian, V. High-Performance Chemical-Bath-Deposited Zinc Oxide Thin-Film Transistors. *IEEE Trans. Electron Devices* **2007**, *54*, 1301–1307.
15. Khallaf, H.; Oladeji, I. O.; Chai, G. Y.; Chow, L. Characterization of CdS Thin Films Grown by Chemical Bath Deposition Using Four Different Cadmium Sources. *Thin Solid Films* **2008**, *516*, 7306–7312.
16. Wang, G. M.; Lu, X. H.; Ling, Y. C.; Zhai, T.; Wang, H. Y.; Tong, Y. X.; Li, Y. LiCl/PVA Gel Electrolyte Stabilizes Vanadium Oxide Nanowire Electrodes for Pseudocapacitors. *ACS Nano* **2012**, *6*, 10296–10302.
17. Alivisatos, A. P. Semiconductor Clusters, Nanocrystals, and Quantum Dots. *Science* **1996**, *271*, 933–937.
18. Hecht, D. S.; Hu, L. B.; Irvin, G. Emerging Transparent Electrodes Based on Thin Films of Carbon Nanotubes, Graphene, and Metallic Nanostructures. *Adv. Mater.* **2011**, *23*, 1482–1513.
19. Wang, D.; Peng, Q.; Li, Y. Nanocrystalline Intermetallics and Alloys. *Nano Res.* **2010**, *3*, 574–580.
20. Liang, H. W.; Cao, X. A.; Zhou, F.; Cui, C. H.; Zhang, W. J.; Yu, S. H. A Free-Standing Pt-Nanowire Membrane as a Highly Stable Electrocatalyst for the Oxygen Reduction Reaction. *Adv. Mater.* **2011**, *23*, 1467–1471.
21. Madaria, A. R.; Kumar, A.; Ishikawa, F. N.; Zhou, C. W. Uniform, Highly Conductive, and Patterned Transparent Films of a Percolating Silver Nanowire Network on Rigid and Flexible Substrates Using a Dry Transfer Technique. *Nano Res.* **2010**, *3*, 564–573.
22. Lin, Z.; Chen, Y.; Yin, A.; He, Q.; Huang, X.; Xu, Y.; Liu, Y.; Zhong, X.; Huang, Y.; Duan, X. Solution Processable Colloidal Nanoplates as Building Blocks for High-Performance Electronic Thin Films on Flexible Substrates. *Nano Lett.* **2014**, *14*, 6547–6553.
23. Duan, X. F. Nanowire Thin-Film Transistors: a New Avenue to High-Performance Macroelectronics. *IEEE Trans. Electron Devices* **2008**, *55*, 3056–3062.
24. Duan, X. F. Assembled Semiconductor Nanowire Thin Films for High-Performance Flexible Macroelectronics. *MRS Bull.* **2007**, *32*, 134–141.
25. Duan, X. F.; Niu, C. M.; Sahi, V.; Chen, J.; Parce, J. W.; Empedocles, S.; Goldman, J. L. High-Performance Thin-Film Transistors Using Semiconductor Nanowires and Nanoribbons. *Nature* **2003**, *425*, 274–278.
26. Kim, D. K.; Lai, Y. M.; Diroll, B. T.; Murray, C. B.; Kagan, C. R. Flexible and Low-Voltage Integrated Circuits Constructed from High-Performance Nanocrystal Transistors. *Nat. Commun.* **2012**, *3*, 1216.
27. Talapin, D. V.; Murray, C. B. PbSe Nanocrystal Solids for n- and p-Channel Thin Film Field-Effect Transistors. *Science* **2005**, *310*, 86–89.
28. Kovalenko, M. V.; Scheele, M.; Talapin, D. V. Colloidal Nanocrystals with Molecular Metal Chalcogenide Surface Ligands. *Science* **2009**, *324*, 1417–1420.
29. Mitzi, D. B. Solution Processing of Chalcogenide Semiconductors via Dimensional Reduction. *Adv. Mater.* **2009**, *21*, 3141–3158.
30. Mitzi, D. B.; Copel, M.; Chey, S. J. Low-Voltage Transistor Employing a High-Mobility Spin-Coated Chalcogenide Semiconductor. *Adv. Mater.* **2005**, *17*, 1285–1289.
31. Hsu, C. J.; Duan, H. S.; Yang, W. B.; Zhou, H. P.; Yang, Y. Benign Solutions and Innovative Sequential Annealing Processes for High Performance Cu<sub>2</sub>ZnSn(Se, S)<sub>4</sub> Photovoltaics. *Adv. Energy Mater.* **2014**, *4*, 1301287.
32. Webber, D. H.; Brutchey, R. L. Alkahest for V<sub>2</sub>V<sub>3</sub> Chalcogenides: Dissolution of Nine Bulk Semiconductors in a Diamine-Dithiol Solvent Mixture. *J. Am. Chem. Soc.* **2013**, *135*, 15722–15725.
33. Webber, D. H.; Buckley, J. J.; Antunez, P. D.; Brutchey, R. L. Facile Dissolution of Selenium and Tellurium in a Thiol-Amine Solvent Mixture under Ambient Conditions. *Chem. Sci.* **2014**, *5*, 2498–2502.
34. Halim, U.; Zheng, C. R.; Chen, Y.; Lin, Z.; Jiang, S.; Cheng, R.; Huang, Y.; Duan, X. A Rational Design of Cosolvent Exfoliation of Layered Materials by Directly Probing Liquid-Solid Interaction. *Nat. Commun.* **2013**, *4*, 2213.
35. Wu, Y.; Wadia, C.; Ma, W. L.; Sadtler, B.; Alivisatos, A. P. Synthesis and Photovoltaic Application of Copper(I) Sulfide Nanocrystals. *Nano Lett.* **2008**, *8*, 2551–2555.
36. Pathan, H. M.; Lokhande, C. D.; Amalnerkar, D. P.; Seth, T. Modified Chemical Deposition and Physico-Chemical Properties of Copper(I) Selenide Thin Films. *Appl. Surf. Sci.* **2003**, *211*, 48–56.
37. Otelaja, O.; Ha, D.; Ly, T.; Zhang, H.; Robinson, R. Highly Conductive Cu<sub>2-x</sub>S Nanoparticle Films through Room-Temperature Processing and an Order of Magnitude Enhancement of Conductivity via Electrophoretic Deposition. *ACS Appl. Mater. Interfaces* **2014**, *6*, 18911–18920.
38. Deka, S.; Genovese, A.; Zhang, Y.; Miszta, K.; Bertoni, G.; Krahn, R.; Giannini, C.; Manna, L. Phosphine-Free Synthesis of p-Type Copper(I) Selenide Nanocrystals in Hot Coordinating Solvents. *J. Am. Chem. Soc.* **2010**, *132*, 8912–8914.
39. Zhang, Y.; Hu, C. G.; Zheng, C. H.; Xi, Y.; Wan, B. Y. Synthesis and Thermoelectric Property of Cu<sub>2-x</sub>Se Nanowires. *J. Phys. Chem. C* **2010**, *114*, 14849–14853.
40. Riha, S. C.; Johnson, D. C.; Prieto, A. L. Cu<sub>2</sub>Se Nanoparticles with Tunable Electronic Properties Due to a Controlled Solid-State Phase Transition Driven by Copper Oxidation and Cationic Conduction. *J. Am. Chem. Soc.* **2011**, *133*, 1383–1390.
41. Shinde, M. S.; Ahirrao, P. B.; Patil, I. J.; Patil, R. S. Thickness Dependent Electrical and Optical Properties of Nanocrystalline Copper Sulphide Thin Films Grown by Simple Chemical Route. *Indian J. Pure Appl. Phys.* **2012**, *50*, 657–660.
42. Ting, C. C.; Lee, W. Y. Cu<sub>2-x</sub>Se Films Fabricated by the Low-Temperature Electrophoretic Deposition. *Electrochem. Solid State Lett.* **2012**, *15*, H1–H4.

43. Cho, A.; Ahn, S.; Yun, J. H.; Gwak, J.; Ahn, S. K.; Shin, K.; Yoo, J.; Song, H.; Yoon, K. The Growth of  $\text{Cu}_{2-x}\text{Se}$  Thin Films Using Nanoparticles. *Thin Solid Films* **2013**, *546*, 299–307.
44. Liu, X.; Wang, X. L.; Zhou, B.; Law, W. C.; Cartwright, A. N.; Swihart, M. T. Size-Controlled Synthesis of  $\text{Cu}_{2-x}\text{E}$  (E = S, Se) Nanocrystals with Strong Tunable Near-Infrared Localized Surface Plasmon Resonance and High Conductivity in Thin Films. *Adv. Funct. Mater.* **2013**, *23*, 1256–1264.
45. Bekenstein, Y.; Vinokurov, K.; Keren-Zur, S.; Hadar, I.; Schilt, Y.; Raviv, U.; Millo, O.; Banin, U. Thermal Doping by Vacancy Formation in Copper Sulfide Nanocrystal Arrays. *Nano Lett.* **2014**, *14*, 1349–1353.
46. Li, X.; Tang, A. W.; Guan, L.; Ye, H. H.; Hou, Y. B.; Dong, G. Y.; Yang, Z. P.; Teng, F. Effects of Alkanethiols Chain Length on the Synthesis of  $\text{Cu}_{2-x}\text{S}$  Nanocrystals: Phase, Morphology, Plasmonic Properties and Dielectrical Conductivity. *RSC Adv.* **2014**, *4*, 54547–54553.
47. Oh, S. J.; Berry, N. E.; Choi, J. H.; Gaulding, E. A.; Lin, H. F.; Paik, T.; Diroll, B. T.; Muramoto, S.; Murray, C. B.; Kagan, C. R. Designing High-Performance PbS and PbSe Nanocrystal Electronic Devices through Stepwise, Post-Synthesis, Colloidal Atomic Layer Deposition. *Nano Lett.* **2014**, *14*, 1559–1566.
48. Milliron, D. J.; Mitzi, D. B.; Cope, M.; Murray, C. E. Solution-Processed Metal Chalcogenide Films for p-Type Transistors. *Chem. Mater.* **2006**, *18*, 587–590.